Available online at www.sciencedirect.com
SCIENCE DIRECT
Dyes and Pigments 70 (2006) 91–98
DYES and PIGMENTS
www.elsevier.com/locate/dyepig

Quantum chemical study on the electronic structure and second-order nonlinear optical properties of salen-type Schiff bases

Iran Sheikhshoaie [a], Walter M.F. Fabian [b,*]

[a] Chemistry Department, Faculty of Science, Shahid-Bahonar University of Kerman, P.O. Box 76175-133, Kerman, Iran
[b] Institut für Chemie, Karl-Franzens Universität Graz, Heinrichstr. 28, A-8010 Graz, Austria

Received 15 March 2005; accepted 12 April 2005
Available online 5 July 2005

Abstract

Semi-empirical (ZINDO-SOS), time-dependent density functional theory and ab initio quadratic response function (DDRPA) calculations on a series of donor–acceptor substituted salen-type Schiff bases are used to aid in the design of dyes with useful optical nonlinearities (molecular quadratic hyperpolarizabilities β_{vec}). 4-Phenylazo-2-phenyliminomethylphenols **1** are calculated to be less suitable as nonlinear optical materials than the isomeric 5-phenylazo-2-phenyliminomethylphenols **2**. The largest hyperpolarizabilities are predicted for compounds with an acceptor-containing phenylazo and a donor-substituted phenyliminomethyl moiety. The calculations also clearly indicate the intramolecular charge transfer nature of the first $\pi\pi^*$-transition in the investigated Schiff bases.

Keywords: Time-dependent density functional theory; Ab initio quadratic response function; Semi-empirical calculations; ZINDO; Electronic excitation energies; Hyperpolarizabilities; Nonlinear optics; Schiff bases

1. Introduction

Aromatic Schiff bases, especially those derived from reaction of salicylic aldehydes with aromatic amines (salen-type Schiff bases), form complexes with a variety of metal ions [1,2]. Among the various possible applications of these complexes [3–7], their nonlinear optical properties for the design of materials in modern communication technology [8–13] are of fundamental importance [14,15]. Besides the experimental determination of macroscopic optical nonlinearities of Schiff base derivatives [16] by the powder technique [17], or their molecular hyperpolarizabilities [18] by electric field induced second harmonic generation (EFISH) [19,20], quantum chemical procedures for the calculations of NLO properties [12,21–26] also have been applied to a series of donor–acceptor substituted Schiff bases [18,27]. Recently, we reported on the synthesis, spectroscopic characterization and semi-empirical AM1 calculations of arylazo substituted salen-type Schiff base ligands [28,29]. Here we present a semi-empirical and ab initio computational study of a series of such salen-type Schiff bases **1**–**4** (Scheme 1) with special emphasis on the influence of the nature (donor vs acceptor) and position of substituents on molecular quadratic hyperpolarizabilities (β_{vec}).

2. Computational details

The geometries of all Schiff bases **1**–**4** (Scheme 1) were optimised using the semi-empirical AM1 Hamiltonian

* Corresponding author. Tel.: +43 316 380 8636; fax: +43 316 380 9840.
E-mail address: walter.fabian@uni-graz.at (W.M.F. Fabian).
URL: http://www.uni-graz.at/walter.fabian

0143-7208/$ - see front matter © 2005 Elsevier Ltd. All rights reserved.
doi:10.1016/j.dyepig.2005.04.011

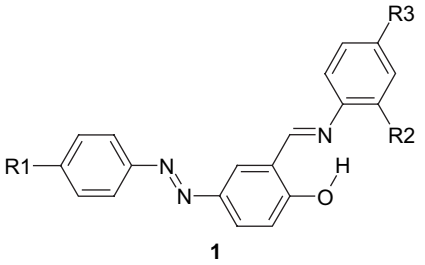

1

1,2	R1	R2	R3
a	H	H	H
b	NO_2	H	OMe
c	OMe	H	NO_2
d	NO_2	OMe	OMe
e	OMe	NO_2	NO_2
f	OMe	OMe	OMe
g	NO_2	NO_2	NO_2
h	NO_2	H	NO_2

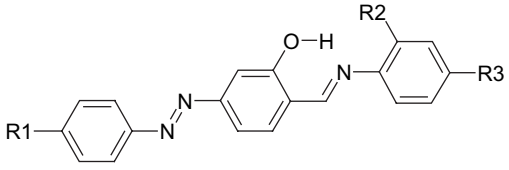

2

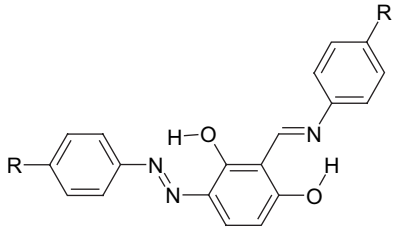

3a: R = H; **3b:** R = NO_2

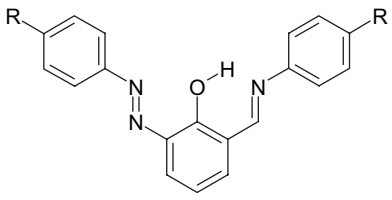

4a: R = H; **4b:** R = NO_2

Scheme 1. Structures of the investigated Schiff bases.

[30,31]. For several selected derivatives (**1a–e**, **2a–e**) geometry optimisation was also done with Becke's three parameter hybrid density functional theory – HF procedure [32] using the Lee–Yang–Parr correlation functional [33] and the 6-31G(d) basis set (B3LYP/6-31G(d)) [34]. Electronic excitation energies and hyperpolarizabilities were obtained by the semi-empirical ZINDO procedure [35,36]. In addition, for **1a–c** and **2a–c**, time-dependent density functional theory (TDDFT [37,38], B3LYP/6-31G(d)) and ab initio HF quadratic response function (double direct random phase approximation, DDRPA) calculations [39,40] with Ahlrichs' VDZ basis [41], were used to obtain electronic excitation energies and hyperpolarizabilities, respectively.

3. Results and discussion

The intramolecular hydrogen bond in **1–4** considerably restricts the conformational freedom. Thus, in **3**, only one single rotamer is possible; the orientation of the azo group with respect to the central aromatic ring in both **1** and **2** leads to two conformers ($\tau_1 = \tau$(C3–C4–N=N) $\sim 0°$ and $\tau_1 \sim 180°$, for atom numbering, see Scheme 1). For molecules with $R^2 \neq H$, each one of these two rotamers leads to two structures depending on the orientation of R^2. Compounds **4a**,**b** may also exist in 4 different conformations (Scheme 2). We will discuss the influence of these conformations on calculated hyperpolarizabilities and electronic transition energies in detail for **1d**, **2d**, and **4a**. Besides the effect of different conformations, other key structural alterations have also been found to influence calculated β-values [42]. Consequently, to address this possibility, we compare ZINDO-SOS calculated quadratic hyperpolarizabilities of **1a–e** and **2a–e** obtained with AM1 and B3LYP/6-31G(d), respectively, geometries.

3.1. Electronic excitation energies

Electronic excitation energies (wavelengths λ/nm), oscillator strengths f, and nature of the respective excited state (principal CI-coefficients) calculated by the TDDFT method for **1a–c** and **2a–c** are summarised in Table 1.

For all derivatives, the calculations predict a very small intensity (low oscillator strength f) for the longest wavelength transition in line with its $n\pi^*$-character. Experimentally, for **1b** and **1d** the UV/vis maxima were

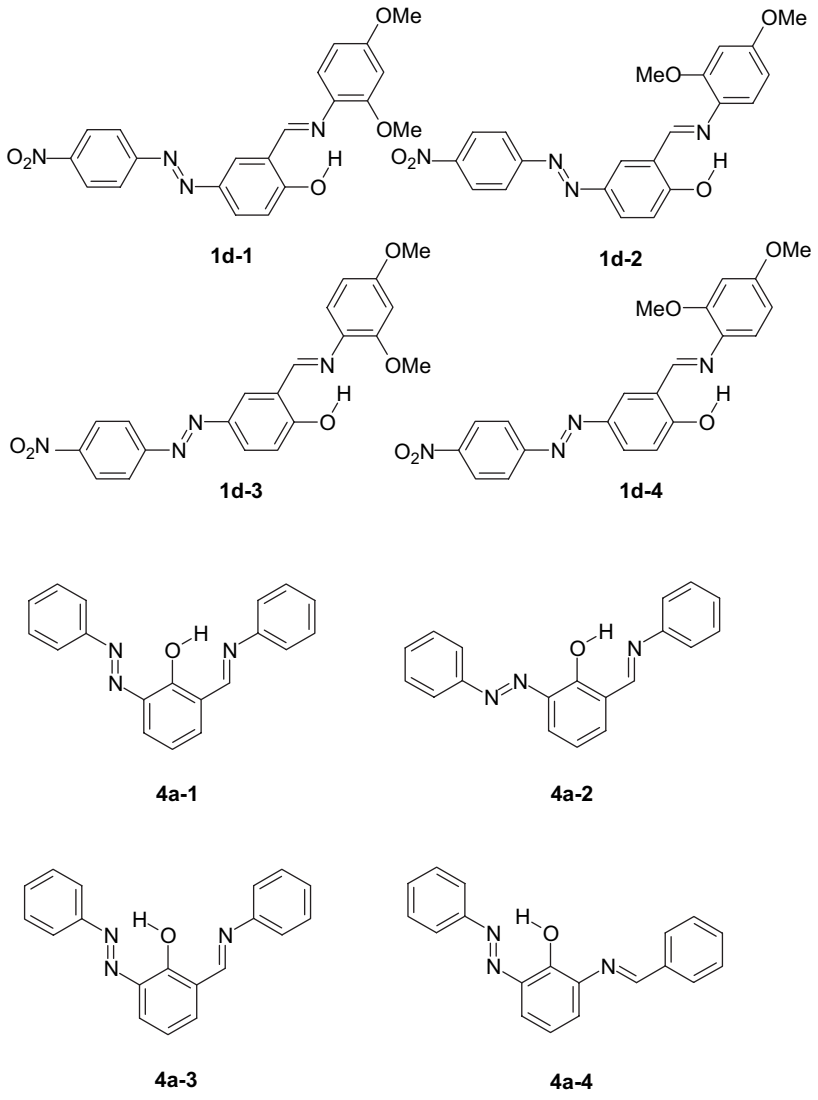

Scheme 2. Conformations of compounds **1d** and **4a**.

found to be λ_{max}(DMF) = 366 and λ_{max}(DMF) = 379 nm, respectively, to be compared with the most intense transitions calculated (TDDFT) for **1b** at 386 nm ($f = 1.166$, Table 1). The corresponding ZINDO values, based on AM1 geometries (Table 2), are 345 (**1b**) and 361 nm (**1d**); those obtained when using B3LYP/6-31G(d) geometries (Table 3), are 374 (**1b**) and 382 nm (**1d**), respectively. From the data given in Table 1, derivatives **2** with *para* arrangement of the phenylazo and the phenyliminomethyl moieties clearly should absorb at longer wavelength than the analogous *meta* isomers **1**. Derivatives with acceptor-substituted phenylazo and donor-substituted phenyliminomethyl groups ($R^1 = NO_2$, $R^3 = CH_3O$, **1b**, **2b**) are predicted to have a bathochromically shifted absorption compared to derivatives with $R^1 = CH_3O$, $R^3 = NO_2$, e.g., **1c**, **2c**). The influence of the substitution pattern on the absorption behaviour of Schiff bases **1** and **2** can easily be understood in terms of the orbitals involved in the respective electronic transitions (Figs. 1 and 2).

For **1a**, the TDDFT calculations predict two close lying transitions (362 nm (HOMO → LUMO+1) and 359 nm (HOMO → LUMO), Table 1) of nearly equal intensity. Both the highest occupied and the lowest virtual orbitals are mainly localized in the azobenzene moiety; the next lowest virtual orbital, LUMO + 1, consists mainly of the Schiff base fragment. These two nearly degenerate transitions, thus, can be considered as intramolecular charge transfer azobenzene → phenyliminomethylbenzene, and locally excited azobenzene → azobenzene transitions, respectively. Introduction of the donor and acceptor groups to give **1b**, lowers the orbital energies of both the HOMO and the LUMO; the former in fact becomes HOMO-1, with the new HOMO (**1b**) mainly localized within the phenyliminomethyl moiety (Fig. 1). As a consequence, the longest wavelength

Table 1
Electronic excitation energies (wavelengths λ/nm), oscillator strengths f, and nature of the respective excited state (principal CI-coefficients) calculated by the TDDFT method for **1a–c** and **2a–c**

Compound	λ/nm	f	CI-vector	
1a	467	0.000	0.64	NHOMO → LUMO
	362	0.503	0.65	HOMO → NLUMO
	359	0.468	0.63	HOMO → LUMO
	342	0.000	0.67	NHOMO → NLUMO
	326	0.582	0.64	HOMO-2 → LUMO
2a	509	0.000	0.65	NHOMO → LUMO
	423	0.555	0.64	HOMO → LUMO
	364	0.552	0.62	HOMO-2 → LUMO
	332	0.373	0.62	HOMO-3 → LUMO
1b	502	0.000	0.65	HOMO-2 → LUMO
	458	0.213	0.67	HOMO → LUMO
	386	1.166	0.61	NHOMO → LUMO
	357	0.274	0.58	HOMO → NLUMO
2b	535	0.002	0.65	HOMO-2 → LUMO
	521	0.556	0.66	HOMO → LUMO
	427	0.060	0.68	NHOMO → LUMO
	365	0.754	0.60	HOMO → NLUMO
1c	459	0.000	0.65	NHOMO → NLUMO
	458	0.109	0.68	HOMO → LUMO
	401	0.000	0.68	NHOMO → LUMO
	374	1.243	0.61	HOMO → NLUMO
2c	513	0.000	0.59	NHOMO → LUMO
	437	1.260	0.64	HOMO → LUMO
	394	0.141	0.62	HOMO-2 → LUMO
	361	0.129	0.61	HOMO → NLUMO

$\pi\pi^*$-absorption can be classified as intramolecular charge transfer transition phenyliminomethylbenzene → azobenzene, i.e. compared to the unsubstituted Schiff base **1a**, this substitution pattern causes a reversal of the donor–acceptor characteristics. The intensity of this transition is calculated to be rather low, because the two orbitals involved are localized in different parts of the molecule with only poor overlap. In contrast, the HOMO-1 is delocalized over the whole molecule, leading to a substantial intensity of the corresponding transition ($f = 1.166$, Table 1). Since the energetic lowering is more pronounced for the virtual orbital (Fig. 1), both transitions are bathochromically shifted compared to those in **1a**. Interchanging the donor and the acceptor group (**1c**, $R^1 = CH_3O$, $R^3 = NO_2$) substantially lowers ε(LUMO + 1), whereas both the HOMO and the LUMO are only slightly affected. In fact, in **1c** the LUMO + 1 of the unsubstituted derivative essentially becomes the lowest virtual orbital (Fig. 1). Again, a substantial red shift of the first transition (359 nm → 458 nm, $f = 0.109$), associated with a low intensity, and a smaller shift for the intense absorption, results (362 nm → 374 nm, $f = 1.243$, Table 1). In contrast to **1a**, a *para* arrangement of the phenylazo and the phenyliminomethyl groups (**2a**), leads to a localization of the HOMO within the phenyliminomethyl moiety rather than the phenylazo group (Fig. 2). The LUMO of **2a** is largely delocalized over the whole molecule and, importantly, is significantly lower than that of **1a** (see Figs 1 and 2), leading to a substantial bathochromic shift of the first $\pi\pi^*$-absorption band in **2a** relative to **1a**. Substitution by donor and acceptor groups ($R^1 = NO_2$, $R^3 = CH_3O$, **2b**) substantially lowers ε(LUMO) and barely affects ε(HOMO) with a concomitant bathochromic shift. The alternate substitution pattern ($R^1 = CH_3O$, $R^3 = NO_2$, **2c**) has a much smaller effect on orbital energies and electronic transition energies (Table 1, Fig. 2). From the topology of the orbitals involved in the longest wavelength $\pi\pi^*$-transition, a significant intramolecular charge transfer character can be inferred (Fig. 2). High NLO responses are intrinsically related to long-wavelength intramolecular charge transfer excited states in push–pull organic π-systems [19,43]. Thus, because of the bathochromic shift predicted for compounds of series **2**, we anticipated enlarged molecular quadratic hyperpolarizabilities compared to those attainable by compounds of series **1**.

3.2. Molecular quadratic hyperpolarizabilities

The quantity actually obtainable from EFISH measurements is $\mu\beta$ (Eq. (1))

$$\mu\beta = \sum_i \mu_i \beta_i \tag{1}$$

where μ_i ($i = x, y, z$) are the vector components of the dipole moment μ with magnitude $||\mu||$, and β_i is defined by (Eq. (2))

$$\beta_i = \beta_{iii} + 1/3 \sum_{j \neq i} \left(\beta_{ijj} + 2\beta_{jji}\right) \tag{2}$$

In the following, to describe the NLO properties of the investigated Schiff bases, the quantity β_{vec} (Eq. (3)), calculated for an excitation energy of $E_{exc} = 1.17$ eV corresponding to the frequency of the commonly used NdYAG laser in EFISH experiments, will be used throughout.

$$\beta_{vec} = \frac{\mu\beta}{||\mu||} \tag{3}$$

$$\beta_{tot} = \left(\sum_i \beta_i^2\right)^{1/2} \tag{4}$$

Note that sometimes β_{vec} (Eq. (3)) is termed β_μ and β_{tot} as defined by Eq. (4), is designated as β_{vec} [44]. Molecular quadratic hyperpolarizabilities β_{vec} calculated by the ZINDO-SOS procedure on the basis of AM1 lowest energy geometries are provided in Table 2,

Table 2
ZINDO results (absorption maxima λ/nm, oscillator strengths f, dipole moments μ/debye, and hyperpolarizabilities β_{vec}) for the lowest energy conformations of the investigated compounds

Compound	λ/nm	f	μ/debye	β_{vec}[a]
1a	529	0.001	2.55	2
	335	0.748		
1b	508	0.005	7.16	40
	377	0.000		
	345	0.879		
1c	524	0.000	8.36	15
	375	0.000		
	344	1.136		
1d	507	0.006	8.01	44
	377	0.000		
	361	0.682		
1e	500	0.000	7.47	19
	379	0.012		
	369	0.000		
	339	1.197		
1f	524	0.000	2.30	6
	361	0.863		
	337	0.740		
1g	497	0.008	6.12	13
	364	0.692		
1h	498	0.006	3.99	14
	376	0.000		
	374	0.000		
	330	0.781		
2a	524	0.007	2.93	−1
	343	0.950		
2b	516	0.016	8.92	55
	377	0.000		
	361	1.070		
2c	504	0.010	8.93	30
	375	0.000		
	345	1.552		
2d	516	0.017	9.91	79
	378	0.879		
2e	497	0.009	7.08	31
	379	0.017		
	370	0.000		
	336	1.360		
2f	520	0.009	3.75	9
	370	1.142		
2g	500	0.015	4.41	0
	372	0.011		
	371	0.003		
	364	0.003		
	331	0.674		
2h	505	0.014	2.45	−3
	376	0.000		
	374	0.000		
	343	0.983		
3a	536	0.000	3.45	−15
	348	0.952		
3b	502	0.005	3.91	7
	376	0.000		
	374	0.000		
	346	1.038		
4a-4	543	0.000	4.27	−5
	350	0.731		
4b	517	0.004	5.17	0
	376	0.000		
	375	0.000		
	348	0.744		

[a] Calculated for an excitation energy $E_{exc} = 1.17$ eV, corresponding to the wavelength emitted by the NdYAG laser ($\lambda = 1064$ nm); in 10^{-30} cm^5/esu.

a comparison of ZINDO results obtained with AM1 vs B3LYP/6-31G(d) structures can be found in Table 3, and the dependence of calculated (ZINDO) β_{vec}-values on molecular conformations is illustrated by the data of Table 4. Hyperpolarizabilities resulting from ab initio Hartree–Fock DDRPA using Ahlrichs' VDZ basis are also listed in Table 3.

The influence of molecular conformation (AM1 geometries) on ZINDO calculated absorption wavelengths λ, dipole moments μ, and hyperpolarizabilities β_{vec} is shown in Table 4. From these data one can infer a negligible effect of the various conformations on the respective NLO properties. Thus, conclusions concerning substituent effects (nature and position) based on the lowest energy conformations are expected to be of sufficient reliability.

As already pointed out above, besides conformation, other key alterations in molecular structure also could significantly affect calculated hyperpolarizabilities [42].

Table 3
Influence of geometry (AM1 vs B3LYP/6-31G(d)) on ZINDO-SOS calculated absorption wavelengths λ, oscillator strengths f, and hyperpolarizabilities β_{vec} (ab initio DDRPA hyperpolarizabilities are given in parentheses)[a]

Compound	AM1 geometry			B3LYP/6-31G(d) geometries		
	λ/nm	f	β_{vec}	λ/nm	f	β_{vec}
1a	335	0.748	2	351	1.332	−13 (−11)
1b	345	0.879	40	374	1.436	77 (85)
1c	344	1.136	15	366	1.558	22 (30)
1d	361	0.682	44	382	1.420	92 (92)
1e	339	1.197	19	369	1.181	21
2a	343	0.950	−1	372	1.111	−2 (−1)
2b	361	1.070	55	399	1.161	94 (81)
2c	345	1.552	30	387	1.685	66 (109)
2d	378	0.879	79	415	1.307	175 (121)
2e	336	1.360	31	380	0.877	56

[a] β_{vec} calculated for an excitation energy $E_{exc} = 1.17$ eV, corresponding to the wavelength emitted by the NdYAG laser ($\lambda = 1064$ nm); in 10^{-30} cm^5/esu.

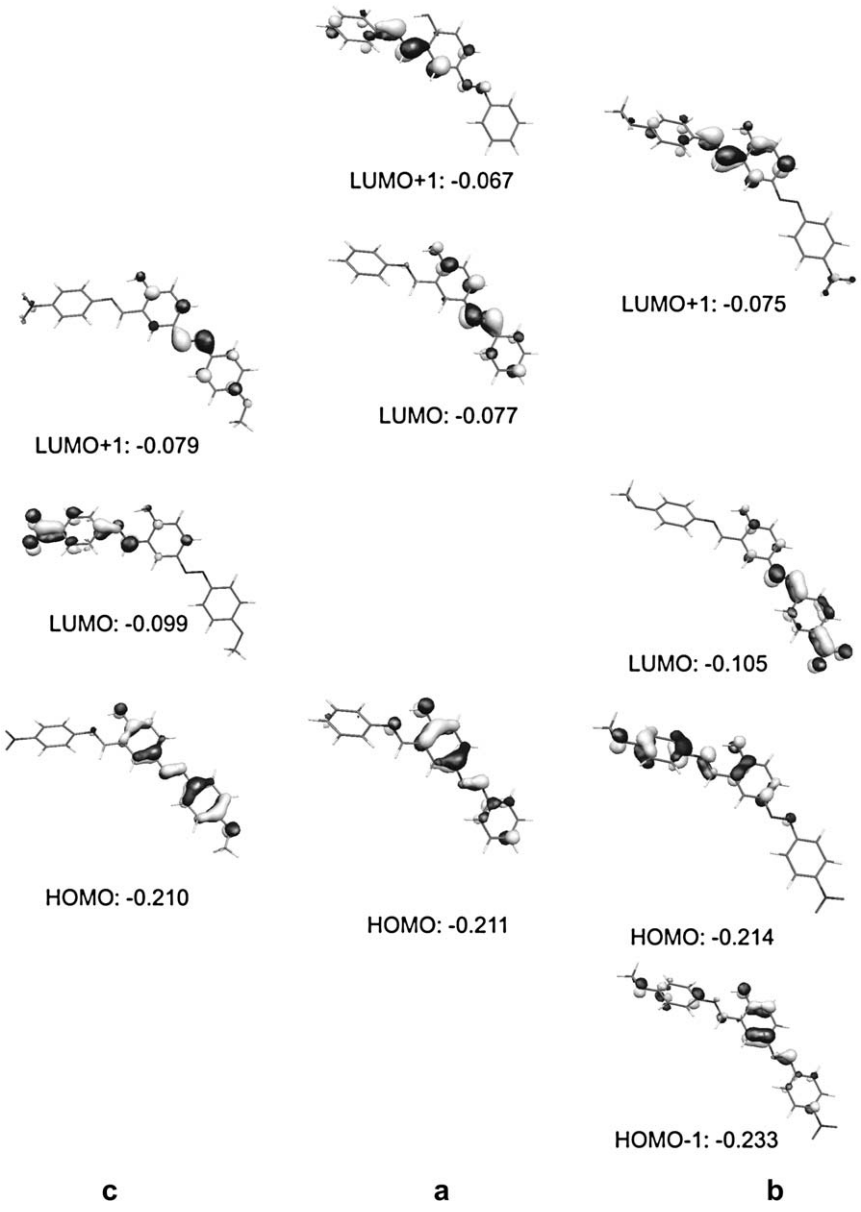

Fig. 1. Plots (MOLEKEL [45,46]) of frontier molecular orbitals of **1a–c**. Orbital energies are given in atomic units.

Using B3LYP/6-31G(d) instead of AM1 structures (Table 3), not only results in calculated longer wavelength absorptions, but also in up to twofold increased hyperpolarizabilities. However, trends resulting from positional isomerism (series **1** vs **2**) as well as the number and position of donor (CH_3O) and acceptor (NO_2) groups, are sufficiently well described when AM1 optimised structures are used. It is also evident that β_{vec} (ZINDO) closely match those obtained by ab initio Hartree–Fock DDRPA calculations (Table 3).

From the data collected in Tables 2 and 3, we can draw the following conclusions: (i) the unsubstituted phenylazo salicylidene anils **1a**, **2a**, **3a**, and **4a** do not show any appreciable NLO response. (ii) In both series **1** and **2**, derivatives with the acceptor attached to the phenylazo and donor to the phenyliminomethyl moiety ($R^1 = NO_2$, $R^3 = CH_3O$, **1b**, **2b**), respectively, have larger β_{vec}-values compared to their isomers with $R^1 = CH_3O$, $R^3 = NO_2$, e.g., **1c**, **2c**). (iii) An additional donor group, $R^2 = CH_3O$, e.g., **1d**, **2d**, leads to a further enhancement of the NLO response. (iv) According to our anticipation, compounds of series **2** have larger molecular quadratic hyperpolarizabilities than the corresponding derivatives of series **1**.

4. Conclusion

A series of salen-type Schiff bases, in particular 4-phenylazo- (**1a–h**) and 5-phenylazo-2-phenyliminomethyl-phenols (**2a–h**), as well as some additional

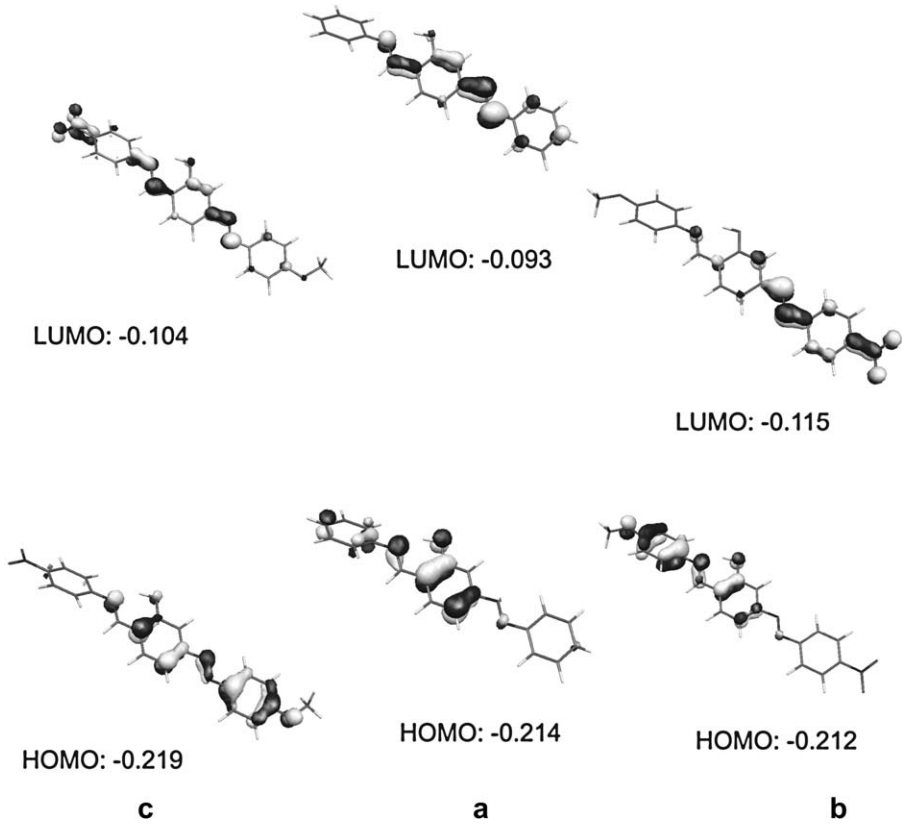

Fig. 2. Plots (MOLEKEL [45,46]) of frontier molecular orbitals of **2a–c**. Orbital energies are given in atomic units.

derivatives, have been investigated by semi-empirical (AM1, ZINDO-SOS), ab initio (HF-DDRPA) quadratic response function and time-dependent density functional (B3LYP) methods. These calculations make possible to rationalize the influence of substituents (position, nature) on UV/vis spectroscopic properties and, especially, on their nonlinear optical response (quadratic molecular hyperpolarizabilities β_{vec}). The most promising candidates for dyes with high optical nonlinearities are donor–acceptor substituted Schiff bases of the series **2** (5-phenylazo-2-phenyliminomethyl-phenols) with the acceptor substituent in *para*-position of the phenylazo- and the donor in *para*- and/or *ortho*, *para*-position of the phenyliminomethyl moiety.

Table 4
Calculated (AM1) heats of formation ΔH_f, ZINDO absorption wavelengths λ, dipole moments μ, and hyperpolarizabilities β_{vec} for different conformations of **1d**, **2d**, and **4a**

Conformation	ΔH_f /kcal mol^{-1}	λ/nm	μ/debye	β_{vec}[a]
1d-1	37.1	358	7.52	45
1d-2	35.2	361	8.01	44
1d-3	38.0	355	7.66	45
1d-4	35.3	359	8.14	44
2d-1	38.9	376	9.96	68
2d-2	37.0	378	9.89	73
2d-3	38.8	375	10.00	73
2d-4	36.9	378	9.91	79
4a-1	110.1	335	2.58	−1
4a-2	110.6	342	2.77	1
4a-3	–[b]			
4a-4	109.1	350	4.27	−5

[a] β_{vec} calculated for an excitation energy $E_{exc} = 1.17$ eV, corresponding to the wavelength emitted by the NdYAG laser ($\lambda = 1064$ nm); in 10^{-30} cm^5/esu.
[b] Collapses to **4a-4**.

References

[1] Hoshino N. Liquid crystal properties of metal–salicylaldimine complexes. Chemical modifications towards lower symmetry. Coord Chem Rev 1998;174:77–108.
[2] Atwood DA, Harvey MJ. Group 13 compounds incorporating salen ligands. Chem Rev 2001;101:37–52.
[3] Cozzi PG. Metal–Salen Schiff base complexes in catalysis: practical aspects. Chem Soc Rev 2004;33:410–21.
[4] Che C-M, Huang J-S. Metal complexes of chiral binaphthyl Schiff-base ligands and their application in stereoselective organic transformations. Coord Chem Rev 2003;242:97–113.
[5] Tsuchida E, Oyaizu K. Oxovanadium(III–V) mononuclear complexes and their linear assemblies bearing tetradentate Schiff base ligands: structure and reactivity as multielectron redox catalysts. Coord Chem Rev 2003;237:213–28.
[6] Binnemans K, Goerller-Walrand C. Lanthanide-containing liquid crystals and surfactants. Chem Rev 2002;102:2303–45.
[7] Menon SK, Jogani SK, Agrawal YK. Macrocyclic schiff bases and their analytical applications. Rev Anal Chem 2000;19:361–412.

[8] Alivisatos AP, Barbara PF, Castleman AW, Chang J, Dixon DA, Klein ML, et al. From molecules to materials: current trends and future directions. Adv Mater 1998;10:1297–336.
[9] Dalton L. Nonlinear optical polymeric materials: from chromophore design to commercial applications. Adv Polym Sci 2002; 158:1–86.
[10] Marder SR, Kippelen B, Jen AKY, Peyghammbarian N. Design and synthesis of chromophores and polymers for electro-optic and photorefractive applications. Nature 1997;388:845–51.
[11] Bosshard C, Wong M-S, Pan F, Spreiter R, Follonier S, Meier U, et al. Novel organic crystals for nonlinear and electrooptics. NATO ASI series, series 3: high technology 1997;24:279–96.
[12] Kanis DR, Ratner MA, Marks TJ. Design and construction of molecular assemblies with large second-order optical nonlinearities. Quantum chemical aspects. Chem Rev 1994;94: 195–242.
[13] Jen AKY, Chen T-A, Rao VP, Cai Y, Liu Y-J, Dalton LR. High performance chromophores and polymers for electro-optic applications. Adv Nonlinear Opt 1997;4:237–49.
[14] Lacroix PG. Second-order optical nonlinearities in coordination chemistry: the case of bis(salicylaldiminato)metal schiff base complexes. Eur J Inorg Chem 2001;339–48.
[15] Di Bella S, Fragala I. Synthesis and second-order nonlinear optical properties of bis(salicylaldiminato)M(II) metalloorganic materials. Synth Met 2000;115:191–6.
[16] Li B, Huang G, Shi L, Liu W, Chen B, Wu X. Preparation, spectroscopy and electrochemistry of some ferrocenyl Schiff base derivatives with NLO responses. Indian J Chem 2003;42B: 2643–8.
[17] Kurtz SK, Perry TT. Powder technique for the evaluation of nonlinear optical materials. J Appl Phys 1968;19:3798–813.
[18] Bhat K, Choi J, McCall SD, Aggarwal MD, Cardelino BH, Moore CE, et al. Theoretical and experimental study of the second-order polarizabilities of Schiff's bases for nonlinear optical applications. Comput Mat Sci 1997;309–16.
[19] Oudar JL. Optical nonlinearities of conjugated molecules. Stilbene derivatives and highly polar aromatic compounds. J Chem Phys 1977;67:446–57.
[20] Levine BF, Bethea CG. Second and third order hyperpolarizabilities of organic molecules. J Chem Phys 1975;63:2666–82.
[21] Morley JO, Pugh D. Computational evaluation of second-order optical nonlinearities. In: Nalwa HS, Miyata S, editors. Nonlinear optics of organic molecules and polymers. Boca Raton: CRC; 1997. p. 29–56.
[22] Morley JO, Pavlides P, Pugh D. On the calculation of the hyperpolarizabilities of organic molecules by the sum over virtual excited states method. Int J Quantum Chem 1992;43:7–26.
[23] Champagne B, Kirtman B. Theoretical approach to the design of organic molecular and polymeric nonlinear optical materials. In: Nalwa HS, editor, Handbook of advanced electronic and photonic materials and devices, vol. 9. San Diego: Academic Press; 2001. p. 63–126.
[24] Zerner MC, Fabian WMF, Dworczak R, Kieslinger DW, Kroner G, Junek H, et al. Nonlinear optical properties of dicyanomethylene-derived heteroaromatic dyes: semiempirical molecular orbital calculations and experimental investigations. Int J Quantum Chem 2000;79:253–66.
[25] Dworczak R, Fabian WMF. Electric field induced second harmonic generation (EFISH) measurements on absorbing compounds: push–pull substituted anilines. Dyes Pigments 2002;53:119–28.
[26] Hrobarik P, Zahradnik P, Fabian WMF. Computational design of benzothiazole-derived push–pull dyes with high molecular quadratic hyperpolarizabilities. Phys Chem Chem Phys 2004;6: 495–502.
[27] Karakas A, Unver H, Elmali A. Schiff bases with various donor–acceptor substituents and regulating groups as non-linear optical materials: ab initio quantum mechanical calculations. Journal of Molecular Structure: THEOCHEM 2004;712:117–22.
[28] Jalali-Heravi M, Khandar AA, Sheikshoaie I. A theoretical investigation of the structure, electronic properties and second-order nonlinearity of some azo Schiff base ligands and their mono anions. Spectrochim Acta A 1999;55A:2537–44.
[29] Jalali-Heravi M, Khandar AA, Sheikshoaie I. Characterisation and theoretical investigation of the electronic properties and second-order nonlinearity of some three dentate salicylaldiminato Schiff base ligands. Spectrochim Acta A 2000;56A:1575–81.
[30] Dewar MJS, Zoebisch EG, Healy EF, Stewart JJP. Development and use of quantum mechanical molecular models. 76. AM1: a new general purpose quantum mechanical molecular model. J Am Chem Soc 1985;107:3902–9.
[31] AMPAC 6.55. © 1999 Semichem, 7128 Summit, Shawnee, KS 66216, USA.
[32] Becke AD. Density-functional thermochemistry III. The role of exact exchange. J Chem Phys 1993;98:5648–52.
[33] Lee C, Yang W, Parr RG. Development of the Colle–Salvetti correlation-energy formula into a functional of the electron density. Phys Rev B 1988;37:785–9.
[34] Frisch MJ, Trucks GW, Schlegel HB, Scuseria GE, Robb MA, Cheeseman JR, et al. Gaussian 03, Revision B.04. Pittsburgh, PA: Gaussian, Inc.; 2003.
[35] Ridley J, Zerner MC. Theor Chim Acta 1973;32:111–34.
[36] Zerner MC. ZINDO, a comprehensive semiempirical quantum chemistry package. Quantum Theory Project. Florida, USA: Gainesville; 1993.
[37] Stratmann RE, Scuseria GE, Frisch MJ. An efficient implementation of time-dependent density-functional theory for the calculation of excitation-energies of large molecules. J Chem Phys 1998;109:8218–24.
[38] Bauernschmitt R, Ahlrichs R. Treatment of electronic excitations within the adiabatic approximation of time dependent density functional theory. Chem Phys Lett 1996;256:454–64.
[39] Agren H, Vahtras O, Koch H, Joergensen P, Helgaker T. Direct, atomic-orbital-based, self-consistent field calculations of nonlinear molecular properties. Application to the frequency-dependent hyperpolarizability of *para*-nitroaniline. J Chem Phys 1993;98: 6417–23.
[40] Helgaker T, Jensen HJAa, Joergensen P, Olsen J, Ruud K, Aagren H, et al. Dalton, a molecular electronic structure program, Release 1.2 2001.
[41] Schäfer A, Horn H, Ahlrichs R. Fully optimized contracted Gaussian basis sets for atoms Li to Kr. J Chem Phys 1992;97: 2571–7.
[42] Kanis DR, Marks TJ, Ratner MA. Calculation of quadratic hyperpolarizabilities for organic π electron chromophores: molecular geometry sensitivity of second order nonlinear optical response. Int J Quantum Chem 1992;43:61–82.
[43] Zyss J. Hyperpolarizabilities of substituted conjugated molecules. III. Study of a family of donor–acceptor disubstituted phenylpolyenes. J Chem Phys 1979;71:909–16.
[44] Varanasi PR, Jen AKY, Chandrasekhar J, Namboothiri INN, Rathna A. The important role of heteroaromatics in the design of efficient second-order nonlinear optical molecules: theoretical investigation on push–pull heteroaromatic stilbenes. J Am Chem Soc 1996;118(49):12443–8.
[45] Flükiger P, Lüthi HP, Portmann S, Weber J. MOLEKEL 4.3. Manno, Switzerland: Swiss Center for Scientific Computing; 2000–2002.
[46] Portmann S, Lüthi HP. MOLEKEL: an interactive molecular graphics tool. CHIMIA 2000;54:766–70.